Dalton Transactions

Accepted Manuscript

This article can be cited before page numbers have been issued, to do this please use: A. schneemann, R. Rudolf, S. Henke, Y. Takahashi, H. Banh, I. Hante, C. Schneider, S. Noro and R. A. A. Fischer, *Dalton Trans.*, 2017, DOI: 10.1039/C7DT01195D.

ROYAL SOCIETY OF CHEMISTRY

rsc.li/dalton

View Article Online
DOI: 10.1039/C7DT01195D

Dalton Transactions

ARTICLE

Linker Functionalisation Triggers an Alternative 3D-Topology for Zn-Isophthalate-4,4'-Bipyridine Frameworks

Received 00th January 20xx,
Accepted 00th January 20xx

DOI: 10.1039/x0xx00000x

www.rsc.org/

Andreas Schneemann,[a,b] Robin Rudolf,[c] Sebastian Henke,[c] Yukiko Takahashi,[d] Hung Banh,[a,b] Inke Hante,[b] Christian Schneider,[a] Shin-ichiro Noro,[d] and Roland A. Fischer[a]*

A series of four Zn^{2+} metal-organic frameworks containing functionalised isophthalate linkers and 4,4'-bipyridine pillars has been prepared and characterised. The isophthalates which contain $–OC_3H_{2n+1}$ alkoxy side chains (with n = 1,2 or 3) form frameworks with a 3D pillared-layer topology instead of the typical 2D layer topology of the renown coordination polymers with an interdigitated structure (CIDs), which is found for shorter $–OC_2H_5$ side chains. The gas adsorption properties of the materials were analysed using N_2, CO_2 and O_2 adsorption measurements at low temperatures.

Introduction

Metal-organic frameworks (MOFs) are porous materials, which are constructed from a metal-containing building block connected by organic linkers.[1-3] These materials show many outstanding properties, *e.g.* ultrahigh surface areas,[4, 5] unprecedented capabilities for designing pore space in a molecular fashion[6-10] and previously unseen structural responsivity.[11-17] The properties can be influenced by different approaches, *e.g.* by the judicious choice of material composition[1] or morphology.[18] Furthermore, controlling the framework topology is a crucial aspect during the preparation of MOFs, since the topology significantly influences the material properties. An interesting example would be the structural isomers MIL-88B[19] and MIL-101.[20] Both frameworks are built from the same metal-clusters and organic linkers, however, they differ in the connectivity of these building blocks, which leads to strikingly contrasting materials properties. MIL-88B shows a massive swelling/shrinking of the cell volume depending on the presence of guest molecules. Contrary, MIL-101 is a very rigid and highly stable framework that features open metal-sites suitable for catalytic reactions under harsh conditions.[21] There are different methods to influence the formation of a certain framework topology. The most straight forward and obvious is the change of reaction conditions. For example, by using a suitable solvent mixture, it is possible to crystallize the $Zn_2(bdc)_2(dabco)$ (bdc = 1,4-benzenedicarboxylate; dabco = diazabicyclo[2.2.2]octane) framework in a kagome lattice pillared-layered structure[22] instead of the commonly observed square-grid structure.[23] Linker functionalisation can also be a tool to control the formation of certain topologies. It has been shown that employing fu-bdc (2,5-functionalized-1,4-benzenedicarboxylate) linkers leads to the formation of a new honeycomb-like topology,[24, 25] contrary to the non-functionalized analogue $Zn_2(bdc)_2(bipy)$ (bipy = 4,4'-bipyridine) which features an interpenetrated square-grid pillared-layered structure.[26]

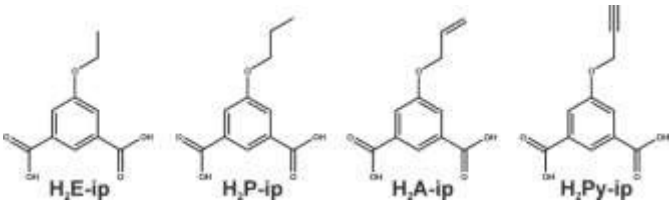

Figure 1: Schematic depiction of the organic linker molecules (and their respective abbreviations) used for the preparation of Zn(fu-ip)(bipy) MOFs.

Within this work we want to present new frameworks of the type Zn(fu-ip)(bipy) (fu-ip = 5-functionalized-isophthalate). Frameworks of the composition Zn(ip)(bipy) have been reported by Kitagawa and coworkers and coined coordination polymers with an interdigitated structure (CIDs).[27, 28] In these frameworks, Zn(ip) 1D chains are interconnected by bipy, forming a 2D sheet with protrusions. The sheets are arranged in an interdigitated fashion to form a 3D structure of layered sheets. Similar compounds have also been reported with other angular linkers (*e.g.* containing functional groups),[29-32] elongated pillars[33] and with other metals (*i.e.* Mn, Fe…).[34, 35] In our approach, we prepared four functionalised linker molecules, namely 5-ethoxyisophthalic acid (H_2E-ip), 5-propoxyisophthalic acid (H_2P-ip), 5-allyloxyisophthalic acid (H_2A-ip) and 5-propynoxyisophthalic acid (H_2Py-ip) which only differ in the chain length and degree of saturation of the side chain (Figure 1). These four linker molecules were used to prepare the frameworks Zn(E-ip)(bipy) (**1**), Zn(P-ip)(bipy) (**2**), Zn(A-ip)(bipy) (**3**) and

[a] Department of Chemistry, Technische Universität München, Lichtenbergstrasse 4, D-85748 Garching, Germany and Catalysis Research Centre, Technische Universität München, Ernst-Otto-Fischer Straße 1, 85748 Garching, Germany
[b] Lehrstuhl für Anorganische Chemie II – Organometallics and Materials, Ruhr Universität Bochum, Universitätsstraße 150, 44801 Bochum, Germany
[c] Anorganische Chemie, Technische Universität Dortmund, Otto-Hahn Straße 6, 44227 Dortmund, Germany
[d] Research Institute for Electronic Science, Hokkaido University, Sapporo 001-0020, Japan

† Electronic Supplementary Information (ESI) available: NMRs, PXRDs (and Pawley Fits), TGAs, IR spectra and Crystallographic Data. CCDC 1540824-1540827. See DOI: 10.1039/x0xx00000x

Zn(Py-ip)(bipy) (**4**) by solvothermal synthesis with $Zn(NO_3)_2 \cdot 6H_2O$ and 4,4'-bipyridine, in a manner similar to the procedures reported in the literature by Nakagawa *et al.* for analogous structures.[28] Following, we discuss the influence of the side chain of the fu-ip linker on the topology and the gas sorption properties of these Zn(fu-ip)(bipy) materials.

Experimental

Linker Synthesis

Dimethyl-5-hydroxyisophthalate

In a 500 mL round-bottom flask 5-hydroxyisophthalic acid (18 g, 87 mmol) and 20 mL $BF_3 \cdot Et_2O$ were dissolved in 400 mL methanol and refluxed overnight. The solvent was evaporated and the remainder was washed several times with cold water to remove BF_3 residues. The obtained yellow solid was dried *in vacuo* at 60 °C overnight. Yield: 78% (14.2 g, 67.6 mmol) ^{1}H-NMR (200 MHz, DMSO-d_6) δ 10.37 (s, 1H), 7.97 (s, 0H), 7.59 (d, J = 1.5 Hz, 2H), 3.89 (s, 6H).

Functionalized Isophthalate Linkers

In a schlenk flask dimethyl-5-hydroxyisophthalate (2 g, 9.5 mmol) and 3 eq K_2CO_3 (3.9 g, 28.5 mmol) were suspended in 60 mL of DMF. Under vigorous stirring. 3 eq of a bromohydrocarbon (see Table S1 and Table S2; ESI) were added dropwise via a syringe. The mixture was heated to 85 °C overnight and afterwards the DMF was removed *in vacuo*. The remainder was suspended in $NaOH_{aq}$ (800 mg in 80 mL deionized water) and refluxed for 4 h. After cooling to room temperature, the mixture was acidified with aqueous HCl and the white precipitate was filtered off and dried *in vacuo*. For yields and NMR data see Table S2 and Section S3 in the ESI.

MOF Synthesis

A 25 mL screw cap bottle was filled with $Zn(NO_3)_2 \cdot 6H_20$ (300 mg, 1.01 mmol) and fu-isophthalic acid linker (H_2E-ip 2.38 mg; H_2P-ip 252 mg; H_2A-ip 250 mg; H_2PY-ip 248 mg; each 1 mmol). The reagents were dissolved in 20 mL DMF via sonication at RT. The solutions were carefully overlaid with 2 mL of a 0.08 mg/mL $bipy_{MeOH}$-stock solution and heated to 70 °C for 48 hours. After cooling to room temperature, the DMF was decanted and replaced by 20 mL fresh DMF and subsequently replaced by 20 mL $CHCl_3$ three times. Afterwards the MOFs were filtered, washed three times with approximately 10 mL of $CHCl_3$, and dried *in vacuo*. Until further manipulation the samples were stored in a glovebox filled with Argon.

Analytical Methods

Liquid phase NMR spectra were recorded on a Bruker Advance DPX 200 spectrometer (^{1}H, 200 MHz) or a Bruker Advance DPX 250 spectrometer (^{1}H, 250 MHz) at 293 K. ^{1}H NMR spectra of the synthesised linker molecules were recorded in DMSO-d_6 and the spectra of digested MOFs were recorded in 0.5 mL DMSO-d_6 and 0.05 mL of DCl/D_2O (20%). Chemical shifts are given relative to TMS and were referenced to the solvent signals as internal standards. **Infrared spectra** were recorded on a Bruker Alpha-P FT-IR situated in a glovebox. For all measurements, the ATR-Mode of the spectrometer was used and measurements were performed with 48 scans. **Thermogravimetric analysis** (TGA) was performed on a Netzsch STA 409 PC TG-DSC apparatus. A heating rate of 5 K/min was applied and the samples were placed in a pre-weighted, clean aluminium oxide crucible. All measurements were performed in a stream of N_2 gas with a constant flowrate of 20 mL/min. **Powder X-ray diffraction** (PXRD) measurements were performed on a PanAlytical X'Pert Pro with Cu Kα Radiation in Bragg-Brentano geometry with an automatic divergence slit and a position sensitive detector while using a continuous scan mode in the range of 2θ = 5° – 50°. The samples were measured on zero-background silicon substrates cut along the [510] plane. For measurements of the as-synthesized samples, the MOF powders were taken straight from the synthesis solution and measured while still slightly wet from the solvent. For measurements of the dried samples, the substrate was covered with a thin film of grease and the dried samples were distributed on the grease. The obtained PXRD patterns were fitted by the Pawley Method[36] using TOPAS academic 4.5. **Gas adsorption** measurements conducted for the samples **2**, **3** and **4** were performed at the Research Institute for Electronical Sciences at Hokkaido University in Sapporo, Japan, using a Belsorp Max adsorption instrument. The samples were filled under ambient conditions into pre-weighted sample tubes. Prior to measurements the samples were evacuated and heated to 120 °C on a Belprep sample preparation station, for the first measurement overnight and for every subsequent measurement for at least three hours. **Single crystal X-ray diffraction** (SCXRD) data were collected on an Agilent Technologies SuperNova diffractometer equipped with an Atlas CCD and multilayer X-ray optics using Cu K_α. The crystals were coated with a perfluoropolyether and picked up with a glass fiber. After mounting, the crystals were slowly cooled from room temperature to the measurement temperature. The obtained data was processed with CrysAlisPro and absorption corrections based on multiple-scanned reflections were carried out with ABSPACK in CrysAlisPro. The crystal structures were solved by direct methods using SHELXS[37] and SUPERFLIP[38] using the OLEX2 interface.[39] After refinement with SHELXL[37] the residual electron density of disordered solvent molecules present in the framework voids was subtracted from the data using the "Solvent Mask" routine of OLEX2.

Results and Discussion

Compounds **1**-**3** yielded crystals suitable for SCXRD measurements (CCDC 1540824-1540826), while the structure of compound **4** could not be solved satisfactorily because of severe twinning of the crystals. However, PXRD clearly demonstrates that **4** is isoreticular to compounds **2** and **3** (see Figure S5, ESI). Interestingly, compounds **2**-**4** crystallise with a different framework topology than compound **1**, which features the renown two-dimensional CID structure**.** In Figure 2a the comparison of the secondary inorganic building units of both

View Article Online
DOI: 10.1039/C7DT01257D

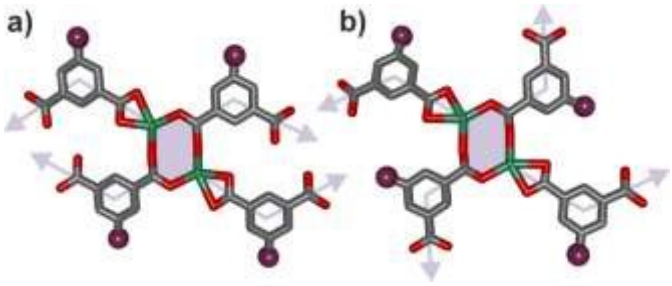

Figure 2: Depiction of the arrangement of the linkers around the inorganic building unit based on an eight membered ring composed of $Zn_2(CO_2)_2$ for compound **1** (a) and compounds **2-4** (b). Carbon atoms are depicted in grey, oxygen in red and zinc in dark green. The functional unit attached to the isophthalates is depicted by purple spheres. Bipy pillars and hydrogen atoms are omitted for clarity.

structure types is displayed. Both building units are composed of an eight-membered ring formed by two carboxylate groups of the fu-ip linkers and two zinc cations. The eight-membered rings are chemically identical and a $Zn_2(fu\text{-}ip)_4$ building block can be identified in both cases. In these building blocks each Zn cation is coordinated by three individual isophthalates. One of those isophthalates is forming an η^2-chelate bond to zinc, occupying two coordination sites. Two isophthalates are bridging two zinc cations, coordinating in a μ-η^1-η^1 fashion. Nevertheless, in both cases the lateral arrangement of the isophthalates within this $Zn_2(fu\text{-}ip)_4$ entity differs. In the case of **1**, a pair of one bridging and one chelating isophthalate form a bridge between two neighbouring eight membered rings. Thus, a one dimensional Zn(fu-ip) chain is formed by double bridging of eight membered $Zn_2(fu\text{-}ip)_4$ rings (Figure 3a). The bipy linker is coordinating to the axial position of the Zn centres, thus stacking the one dimensional chains to form a 2D sheet of the composition Zn(fu-ip)(bipy). Adjacent sheets are stacked onto each other, interacting only by weak intramolecular interactions to yield a layered material (Figure 3c). As expected, this structure (compound **1**) is completely analogous to the isophthalate based CID frameworks introduced by Kitagawa and co-workers. [27, 28]

In case of **2-4**, the local structure around the eight-membered ring differs, which in turn leads to a different global structure and topology of the framework. In these compounds the same $Zn_2(fu\text{-}ip)_4$ units exist, however, the bridging isophthalates are rotated by 180° along their C_{Ar}-$C_{Carboxylate}$ axis. This means, all four isophthalates in the $Zn_2(fu\text{-}ip)_4$ entity of **2-4** are pointing in different directions, thus connecting each eight-membered ring with four neighbouring eight-membered rings (Figure 3b). This kind of connectivity among the eight membered rings results in a Zn(fu-ip) 2D sheet structure with a distorted **sql** topology. Bipy pillars stack these sheets on top of each other resulting in a 3D pillared-layered framework (Figure 3d).

Our findings indicate that the steric bulk of the side chain influences the arrangement of fu-ip linkers around the inorganic building unit, which in turn has a pronounced influence on the framework topology. However, tuning the synthesis conditions might lead to the formation of the denser CID structures also with linkers containing longer side chains. A recent report by Wu *et al.* underlines the influence of reaction time and temperature on the crystallisation and interconversion of polymorphous, but differently dense, phases of related pillared-layered MOFs.[40, 41] In fact on one occasion, for Zn(P-ip)(bipy), single crystals exhibiting the CID structure were obtained, however, this result was not reproducible and seems to be a serendipitous result (see ESI for details; CCDC 1540827). Interestingly, the crystal structure of the Zn(P-ip)(bipy) framework in the CID structure reveals a crystallographic density of 1.233 g/cm^3 which is substantially higher than the density of the corresponding pillared-layered phase (0.984 g/cm^3, the densities represent skeletal densities, neglecting any guest molecule in the pores). It is sensible that the more dense CID phase should preferentially form because of thermodynamic reasons, however, this does not seem to be the case here. We strongly assume that by tuning the synthesis conditions, both phases, the pillared-layered as well as the CID phase, are accessible. In fact, it is likely that the linkers featuring small (or even no) side groups on the isophthalate backbone, previously reported by Kitagawa *et al.*,[27, 28] also can form a pillared-layered network instead of the CID structure.

In order to assess the porosity of compounds **2-4**, the synthesis solvent guests were removed by solvent exchange followed by evacuation at elevated temperatures. Complete solvent removal was verified by ^{1}H NMR spectroscopy and TGA (ESI). Phase purity and structural integrity after activation was confirmed using powder X-ray diffraction (PXRD) of grinded powders of the samples (ESI).

The pore apertures in materials **2-4** are very small and each channel is gated by neighbouring -OC_3H_{2n+1} chains. In previous studies we were already able to show the striking effect that pendent side chains have on the gas adsorption properties of flexible as well as rigid MOFs.[1, 12, 24, 25, 42, 43] Thus, low temperature adsorption isotherms were performed on compounds **2-4** for N_2, O_2 (all at 77 K) and CO_2

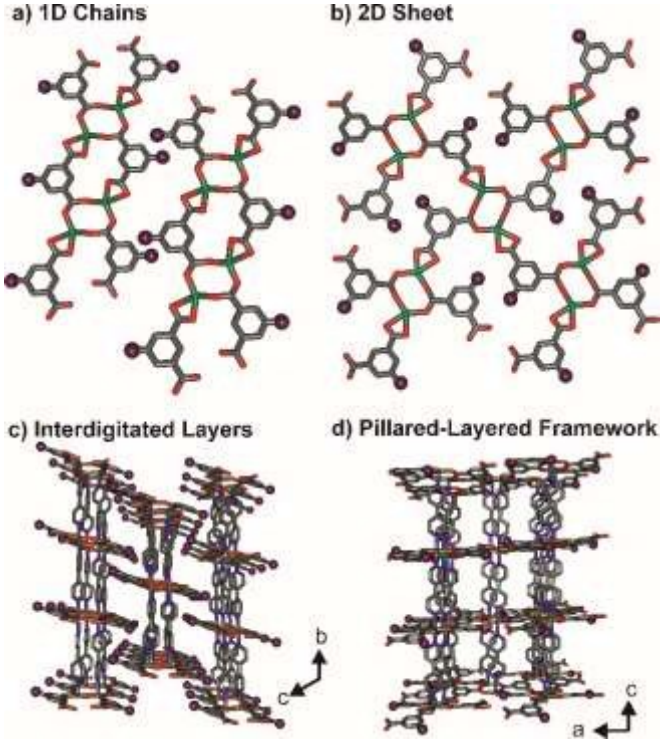

Figure 3: Illustration of the crystal structures of materials **1-4**. Representation of two adjacent 1D chains formed in compound **1** (a) and the 2D sheets formed in compounds **2-4** (b). Depiction of the interdigitated layers in compound **1**, viewed along the *a*-axis (c) and the pillared layers in compounds **2-4** viewed along the *b* axis (d). Carbon atoms are represented in grey, oxygen in red, nitrogen in blue and zinc in dark green. The functionalised side chains are represented by purple spheres. Hydrogen atoms are omitted for the sake of clarity.

View Article Online
DOI: 10.1039/C7DT01195D

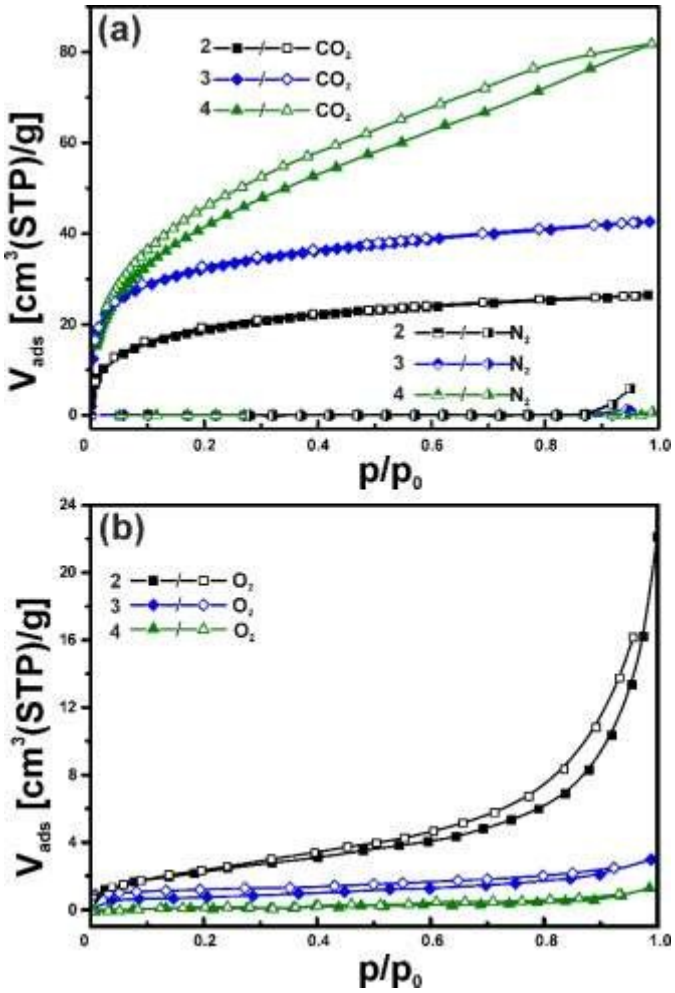

Figure 4: Gas adsorption and desorption isotherms for materials **2**, **3** and **4** are depicted as black squares, blue diamonds and green triangles respectively. CO_2 sorption isotherms (a) were measured at 195 K, N_2 (a) and O_2 (b) at 77 K. P_0 for O_2 is 16.69 kPa at 77 K. The lines indicate a guide to the eye only.

(at 195 K) (Figure 4). All three materials have a negligible uptake of N_2, while the CO_2 uptake varies with the utilised side chain pinned to the ip-linker. Material **2** contains a completely saturated propoxy side chain and has the smallest CO_2 uptake at p/p_0 = 1 and 195 K (~26 cm^3/g), **3** containing additional unsaturated sites on the appendant side chain takes up considerably larger amounts of CO_2 (~43 cm^3/g). The highest CO_2 uptake can be found for **4**, which has triple bonds present in the side chain (~81 cm^3/g). The amount of CO_2 adsorbed at p/p_0 = 1 depends (nearly linearly) on the degree of saturation of the side chain, whereby the lower the degree of saturation of the side chain, the higher the overall CO_2 uptake. In a previous report on the adsorption of vapours in similarly functionalised copper frameworks,[44] the flexibility of the side chains (*i.e.* their probability of occupying different positions due to their rotational degrees of freedom) caused the differences in uptake and the fully saturated framework showed the highest guest adsorption. In contrast, within our study, the framework with the most rigid functionality, namely **4**, shows the highest uptake. This leads to the conclusion that the CO_2 adsorption increases with higher dispersive interactions of the unsaturated side chains with the guest molecules. Note that the slight hysteresis in the adsorption isotherm of **4** is due to a kinetically hindered desorption process. The exact opposite trend can be found for the oxygen adsorption. The highest uptake can be found for material **2** containing propoxy chains. The materials containing double and triple bonds on the linker side chains have considerably lower uptakes. This result is not surprising as saturated hydrocarbons also tend to dissolve oxygen better than unsaturated hydrocarbons.[45] However, it should also be noted that the overall adsorbed amount of oxygen is quite low in all three cases.

Conclusions

We were able to prepare a 3D pillared-layered topology for MOFs of the type Zn(fu-ip)(bipy) by linker functionalisation. We rationalise the formation of the 3D frameworks instead of the typical 2D layer structure on the basis of the pore space available to host DMF solvent molecules during synthesis. The novel materials feature very narrow 2D-connected channels, which are partially populated by alkoxy side chains. The degree of saturation of these side chains has a profound impact on the sorption properties of these materials. Future studies, which are currently under development, will feature the analysis of these materials towards the adsorption of hydrocarbons and the effect of new side chains on the formed framework topology and adsorption properties.

Acknowledgement

A. S. gratefully acknowledges the Ruhr University Research School PLUS for a travel grant to conduct experiments at the Research Center for Electronic Sciences at Hokkaido University, Japan. Ruhr University Research School PLUS is funded by Germany's Excellence Initiative [DFG-GSC 98/3]. This work is supported by the Cluster of Excellence RESOLV (EXC 1069, https://ruhr-uni-bochum.de/solvation) funded by the Deutsche Forschungsgemeinschaft (DFG). The authors gratefully acknowledge Dr. Stephen R. Hughes (DST Innovations, Bridgend, United Kingdom) for proof reading the manuscript.

Notes and references

1. A. Schneemann, S. Henke, I. Schwedler and R. A. Fischer, *ChemPhysChem*, 2014, **15**, 823-839.
2. A. G. Slater and A. I. Cooper, *Science*, 2015, **348**, 988.
3. J. Jiang, Y. Zhao and O. M. Yaghi, *J. Am. Chem. Soc.*, 2016, **138**, 3255-3265.
4. P. Deria, D. A. Gomez-Gualdron, W. Bury, H. T. Schaef, T. C. Wang, P. K. Thallapally, A. A. Sarjeant, R. Q. Snurr, J. T. Hupp and O. K. Farha, *J. Am. Chem. Soc.*, 2015, **137**, 13183-13190.
5. T. C. Wang, W. Bury, D. A. Gomez-Gualdron, N. A. Vermeulen, J. E. Mondloch, P. Deria, K. Zhang, P. Z. Moghadam, A. A. Sarjeant, R. Q. Snurr, J. F. Stoddart, J. T. Hupp and O. K. Farha, *J. Am. Chem. Soc.*, 2015, **137**, 3585-3591.
6. N. T. T. Nguyen, H. Furukawa, F. Gandara, H. T. Nguyen, K. E. Cordova and O. M. Yaghi, *Angew. Chem., Int. Ed.*, 2014, **53**, 10645-10648.

7. B. Li, H.-M. Wen, Y. Cui, W. Zhou, G. Qian and B. Chen, *Adv. Mater.*, 2016, **28**, 8819-8860.
8. X. Zhao, X. Bu, E. T. Nguyen, Q.-G. Zhai, C. Mao and P. Feng, *J. Am. Chem. Soc.*, 2016, **138**, 15102-15105.
9. A. M. Fracaroli, P. Siman, D. A. Nagib, M. Suzuki, H. Furukawa, F. D. Toste and O. M. Yaghi, *J. Am. Chem. Soc.*, 2016, **138**, 8352-8355.
10. S. Yuan, Y.-P. Chen, J.-S. Qin, W. Lu, L. Zou, Q. Zhang, X. Wang, X. Sun and H.-C. Zhou, *J. Am. Chem. Soc.*, 2016, **138**, 8912-8919.
11. M. K. Taylor, T. Runcevski, J. Oktawiec, M. I. Gonzalez, R. L. Siegelman, J. A. Mason, J. Ye, C. M. Brown and J. R. Long, *J. Am. Chem. Soc.*, 2016, **138**, 15019-15026.
12. A. Schneemann, Y. Takahashi, R. Rudolf, S.-i. Noro and R. A. Fischer, *J. Mater. Chem. A*, 2016, **4**, 12963-12972.
13. K. Roztocki, D. Jedrzejowski, M. Hodorowicz, I. Senkovska, S. Kaskel and D. Matoga, *Inorg. Chem.*, 2016, **55**, 9663-9670.
14. J. Pang, C. Liu, Y. Huang, M. Wu, F. Jiang, D. Yuan, F. Hu, K. Su, G. Liu and M. Hong, *Angew. Chem., Int. Ed.*, 2016, **55**, 7478-7482.
15. S. Krause, V. Bon, I. Senkovska, U. Stoeck, D. Wallacher, D. M. Toebbens, S. Zander, R. S. Pillai, G. Maurin, F.-X. Coudert and S. Kaskel, *Nature*, 2016, **532**, 348-352.
16. S.-m. Hyun, J. H. Lee, G. Y. Jung, Y. K. Kim, T. K. Kim, S. Jeoung, S. K. Kwak, D. Moon and H. R. Moon, *Inorg. Chem.*, 2016, **55**, 1920-1925.
17. M. L. Foo, R. Matsuda, Y. Hijikata, R. Krishna, H. Sato, S. Horike, A. Hori, J. Duan, Y. Sato, Y. Kubota, M. Takata and S. Kitagawa, *J. Am. Chem. Soc.*, 2016, **138**, 3022-3030.
18. S. Furukawa, J. Reboul, S. Diring, K. Sumida and S. Kitagawa, *Chem. Soc. Rev.*, 2014, **43**, 5700-5734.
19. C. Serre, C. Mellot-Draznieks, S. Surble, N. Audebrand, Y. Filinchuk and G. Ferey, *Science*, 2007, **315**, 1828-1831.
20. G. Ferey, C. Mellot-Draznieks, C. Serre, F. Millange, J. Dutour, S. Surble and I. Margiolaki, *Science*, 2005, **309**, 2040-2042.
21. A. Santiago-Portillo, S. Navalón, F. G. Cirujano, F. X. L. i. Xamena, M. Alvaro and H. Garcia, *ACS Catalysis*, 2015, **5**, 3216-3224.
22. H. Chun and J. Moon, *Inorg. Chem.*, 2007, **46**, 4371-4373.
23. D. N. Dybtsev, H. Chun and K. Kim, *Angew. Chem., Int. Ed.*, 2004, **43**, 5033-5036.
24. S. Henke and R. A. Fischer, *J. Am. Chem. Soc.*, 2011, **133**, 2064-2067.
25. S. Henke, A. Schneemann, S. Kapoor, R. Winter and R. A. Fischer, *J. Mater. Chem.*, 2012, **22**, 909-918.
26. B. Chen, C. Liang, J. Yang, D. S. Contreras, Y. L. Clancy, E. B. Lobkovsky, O. M. Yaghi and S. Dai, *Angew. Chem., Int. Ed.*, 2006, **45**, 1390-1393.
27. S. Horike, D. Tanaka, K. Nakagawa and S. Kitagawa, *Chem. Commun.*, 2007, 3395-3397.
28. K. Nakagawa, D. Tanaka, S. Horike, S. Shimomura, M. Higuchi and S. Kitagawa, *Chem. Commun.*, 2010, **46**, 4258-4260.
29. D. Tanaka, K. Nakagawa, M. Higuchi, S. Horike, Y. Kubota, T. C. Kobayashi, M. Takata and S. Kitagawa, *Angew. Chem., Int. Ed.*, 2008, **47**, 3914-3918.
30. T. Fukushima, S. Horike, Y. Inubushi, K. Nakagawa, Y. Kubota, M. Takata and S. Kitagawa, *Angew. Chem., Int. Ed.*, 2010, **49**, 4820-4824.
31. H. Sato, R. Matsuda, K. Sugimoto, M. Takata and S. Kitagawa, *Nat. Mater.*, 2010, **9**, 661-666.
32. M. Inukai, T. Fukushima, Y. Hijikata, N. Ogiwara, S. Horike and S. Kitagawa, *J. Am. Chem. Soc.*, 2015, **137**, 12183-12186.
33. Y. Hijikata, S. Horike, M. Sugimoto, H. Sato, R. Matsuda and S. Kitagawa, *Chem. - Eur. J.*, 2011, **17**, 5138-5144.
34. C. Ma, C. Chen, Q. Liu, D. Liao, L. Li and L. Sun, *New J. Chem.*, 2003, **27**, 890-894.
35. M.-H. Zeng, X.-L. Feng and X.-M. Chen, *Dalton Trans.*, 2004, 2217-2223.
36. G. S. Pawley, *J. Appl. Crystallogr.* , 1981, **14**, 357-361.
37. G. M. Sheldrick, *Acta Crystallogr., Sect. C: Struct. Chem.*, 2015, **71**, 3-8.
38. L. Palatinus and G. Chapuis, *Journal of Applied Crystallography*, 2007, **40**, 786-790.
39. O. V. Dolomanov, L. J. Bourhis, R. J. Gildea, J. A. K. Howard and H. Puschmann, *J. Appl. Crystallogr.*, 2009, **42**, 339-341.
40. Y. Wu, S. Henke, G. Kieslich, I. Schwedler, M. Yang, D. A. X. Fraser and D. O'Hare, *Angew. Chem., Int. Ed.*, 2016, **55**, 14081-14084.
41. H. H. M. Yeung, Y. Wu, S. Henke, A. K. Cheetham, D. O'Hare and R. I. Walton, *Angew. Chem., Int. Ed.*, 2016, **55**, 2012-2016.
42. A. Schneemann, E. D. Bloch, S. Henke, P. L. Llewellyn, J. R. Long and R. A. Fischer, *Chem. - Eur. J.*, 2015, **21**, 18764-18769.
43. S. Henke, A. Schneemann, A. Wuetscher and R. A. Fischer, *J. Am. Chem. Soc.*, 2012, **134**, 9464-9474.
44. Y. Sha, S. Bai, J. Lou, D. Wu, B. Liu and Y. Ling, *Dalton Trans.*, 2016, **45**, 7235-7239.
45. R. Battino, T. R. Rettich and T. Tominaga, *J. Phys. Chem. Ref. Data*, 1983, **12**, 163-178.

View Article Online
DOI: 10.1039/C7DT01195D

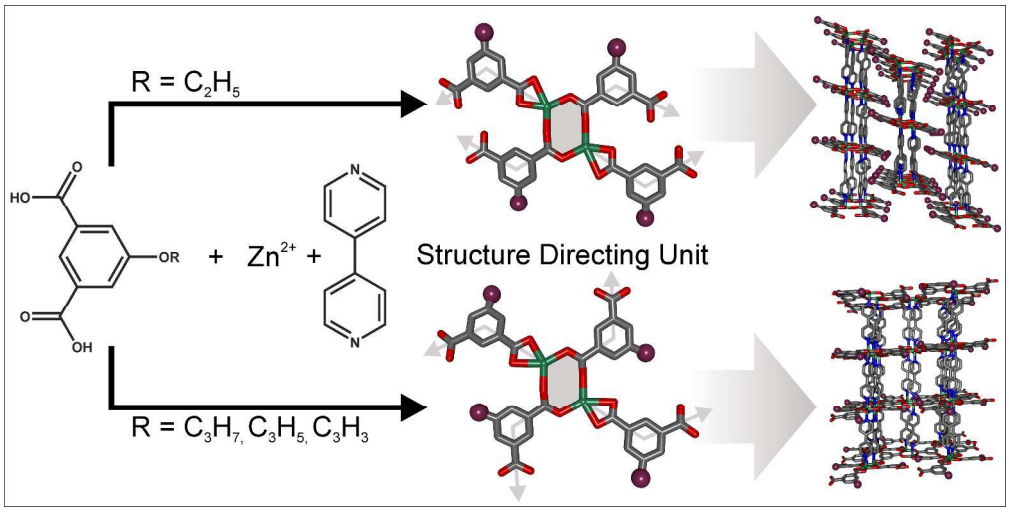

423x211mm (300 x 300 DPI)